Computer Simulations of Cyclic and Acyclic Cholinergic Agonists: Conformational Search and Molecular Dynamics Simulations

Kathleen A. McGroddy,* John W. Brady,‡ and Robert E. Oswald*

* Department of Pharmacology, College of Veterinary Medicine, and ‡Department of Food Science, College of Agriculture and Life Sciences, Cornell University, Ithaca, New York 14853 USA

ABSTRACT Molecular dynamics simulations have been performed on aqueous solutions of two chemically similar nicotinic cholinergic agonists in order to compare their structural and dynamical differences. The cyclic 1,1-dimethyl-4-acetylpiperazinium iodide (HPIP) molecule was previously shown to be a strong agonist for nicotinic acetylcholine receptors (McGroddy et al., 1993), while the acyclic *N,N,N,N'*-tetramethyl-*N'*-acetylethylenediamine iodide (HTED) derivative is much less potent. These differences were expected to arise from differences in the solution structures and internal dynamics of the two molecules. HPIP was originally thought to be relatively rigid; however, molecular dynamics simulations suggest that the acetyl portion of the molecule undergoes significant ring dynamics on a psec timescale. The less constrained HTED molecule is relatively rigid, with only one transition observed about any of the major dihedrals in four 100 psec simulations, each started from a different conformation. The average structures obtained from the simulations are very similar to the starting minimized structure in each case, except for the HTED simulation where a single rotation about the N—C—C—N(+) backbone occurred. In each case, HTED had three to five more water molecules in its primary solvation shell than HPIP, indicating that differences in the energetics of desolvation before binding may partially explain the increased potency of HPIP as compared to HTED.

In the absence of an accurate description of the local environment of the agonist binding site, the molecular analysis of receptor-ligand interactions is made more difficult. In order to investigate these interactions, it is common to search for similar features, or pharmacophores, between compounds which are able to bind to and activate the receptor of interest. Such an approach has often been used in the study of molecules which are able to bind to the nicotinic acetylcholine receptors (nAChRs) and lead to the opening of a nonspecific cation channel. The pharmacophore which has been reliably used for this system was developed from the work of Beers and Reich (1970), who described the requirements for an agonist as consisting of a positive charge distribution separated from a hydrogen bond acceptor by approximately 5.9 Å. This has been shown to be a necessary but not sufficient criterion to predict agonist potency. Many molecules have been synthesized in order to find a more rigid template for agonists than the flexible acetylcholine (ACh) molecule (Gund et al., 1986; Spivak et al., 1986; Spivak et al., 1989). One of these is 1,1-dimethyl-4-acetyl-piperazinium iodide (HPIP), shown in Fig. 1 *A*, which has been shown to bind to and activate the receptor in a manner essentially indistinguishable from acetylcholine but with slightly lower affinity (McGroddy et al., 1993).

Since the potency of the more constrained HPIP is similar to that of ACh, it was of interest to determine the effects of increasing the degrees of freedom of the HPIP molecule. The acyclic derivative of HPIP, *N,N,N,N'*-tetramethyl-*N'*-acetylethylenediamine iodide (HTED, see Fig. 1 *A*) was synthesized to explore this idea further. HTED is chemically similar to ACh except for the replacement of the ester oxygen in ACh by an amide nitrogen which has a methyl substituent not present in ACh. Despite these similarities, HTED has been shown to be from 10–1000 fold less potent than HPIP (and by extension ACh), depending upon the assay (McGroddy et al., 1993). These potency differences are partially due to the fact that the HTED molecule exists in two energetically different structures in solution, due to rotation about the amide bond. The energy barrier to interconversion is high (~19 kcal/mol) so that the isomerization is slow at room temperature, with a rate constant of approximately 0.01 sec^{-1}(McGroddy and Oswald, 1993). Only the less stable *cis* conformer[1] appears to be able to interact with the receptor (McGroddy et al., 1993). In addition, the orientation of the N—C—C—N(+) backbone dihedral angle (O—C—C—N(+) in ACh) is thought to be important for biological activity, although there has been some controversy as to whether it is GAUCHE (60°) or TRANS (180°) in the bound state conformation (Behling et al., 1988; Wilson et al., 1991). It was expected that another factor which could potentially contribute to differences in potency would be entropy, since HPIP was expected to be a relatively rigid molecule, while HTED could potentially access a large number of rotameric states in solution. This could lead to a greater loss of entropy upon the binding of HTED to the nAChRs as compared to the binding of HPIP. Finally, solvation differ-

Received for publication 27 May 1993 and in final form 8 November 1993.

Address reprint requests to Dr. Robert E. Oswald, Department of Pharmacology, College of Veterinary Medicine, Cornell University, Ithaca, NY 14853. Tel.: 607-253-3877; Fax: 607-253-3659.

Abbreviations used: HPIP, 1,1-dimethyl-4-acetylpiperazinium iodide; HTED, *N,N,N,N'*-tetramethyl-*N'*-acetylethylene-diamine iodide; nAChR, nicotinic acetylcholine receptor; *c*G, *cis* GAUCHE; *c*G⁻, *cis* GAUCHE⁻; *c*T, *cis* TRANS; $r_{B\text{-}R}$, Beers-Reich distance (distance between the amine nitrogen and the *van der Waals* extension of the carbonyl oxygen); *t*G, *trans* GAUCHE; *t*G⁻, *trans* GAUCHE⁻; and *t*T, *trans* TRANS.

0006-3495/94/02/314/11 $2.00

[1] *cis* and *trans* refer to the orientation about the amide dihedral, while TRANS and GAUCHE describe the N—C—C—N(+) backbone) see Fig. 1 *B* for structures).

ences could play a role in the energetics of binding. Molecular dynamics simulations were undertaken as a means of studying these factors.

MATERIALS AND METHODS

Energy minimization and molecular dynamics simulations were performed on a Silicon Graphics Iris 4D/220GTX using CHARMm 21.2 (Molecular Simulations, Inc.). The parameters used were from the Polygen Parm30 set, and atomic charges were obtained from the work of Jorgensen et al. (Jorgensen and Gao, 1986; Jorgensen and Swenson, 1985) on small model compounds. Since all of the hydrogen atoms in these molecules were explicitly included, the Jorgensen extended atom charges were distributed among the methyl and methylene groups consistent with results obtained from semi-empirical molecular orbital calculations on these molecules (K.A. McGroddy, unpublished results using MOPAC; Dewar and Zoebisch, 1988; Dewar et al., 1985). The charge distribution is shown in Fig. 1 *A*. The coordinates obtained from the semi-empirical study were used as starting points for these calculations. Each system consisted of one drug molecule solvated by 499 TIP3P water molecules (Jorgensen et al., 1983) in a cube with boxlength 24.7671 Å, using periodic boundary conditions. Long range nonbonded interactions were handled on an atom-by-atom basis and were truncated using a shifting potential function with a cutoff distance of 12 Å (Tasaki et al., 1993). To begin the simulation, an energy-minimized solute molecule was placed in the center of a previously equilibrated box of 512 TIP3P water molecules and all overlapping solvent molecules were removed. The system then underwent 50 steps of steepest descent minimization to remove any bad contacts. Following minimization, the system was equilibrated for 16 psec, with rescaling of the velocities if the temperature, averaged over 1 psec, deviated from 300 K by more than ± 3K. A 100 psec trajectory was then generated in the microcanonical ensemble for each system, using a time step of 1 fsec. All bonds containing hydrogen atoms were constrained by the SHAKE algorithm (Ryckaert et al., 1977; van Gunsteren and Berendsen, 1977). The total energies of the simulations were well conserved, so that kinetic energies were not rescaled during the 100 psec trajectory. The coordinates and velocities were saved every 5 steps for further analysis. Trajectories were analyzed both with programs developed locally and with CHARMm. The *trans/cis* equilbrium constant was determined from the average energies by calculating the population of each conformer relative to the lowest energy conformer according to the Boltzmann distribution.

RESULTS

Conformational search

Single channel recording and radioligand binding experiments were previously used to quantitate the differences in potency between HPIP and HTED (McGroddy et al., 1993). These results indicated that the most important factor in the initial recognition of the drug by the nAChRs is the solution conformation of the agonist, particularly the orientation about the amide bond in HTED (since HPIP is symmetric with respect to rotation about the amide bond). HTED exists in two different solution conformations, one of which is favored by 6.1-fold over the other. ^{19}F NMR experiments suggest that only the less stable *cis* HTED conformer (see Fig. 1 *A*) is able to interact with the nAChR from *Torpedo* electroplaque (McGroddy et al., 1993). In order to obtain more information about the accessible rotameric states of HTED, a conformational search was performed using dielectrics (ϵ) of 1, r (distance-dependent dielectric), and 80. The amide torsion angle was varied from 0° to 360° in 10° increments, while each of the two relevant backbone dihedrals (C—N-(amide)—C—C and N—C—C—N(+)) was rotated in three 120° increments. This gave a total of 6 starting geometries for each value of the amide torsion. At each step, a large (500 kcal/mol) force constant was applied to the amide torsion to keep it near the starting value. The geometry was then optimized to a gradient of 0.01 kcal/mol·Å using the conjugate gradient method. The minimum energies of the most populated conformers are shown in Table 1 and the minimized structures are shown in Fig. 1 *B*.

Amide bond

For all three values of the dielectric, the *trans* (amide methyl *trans* to carbonyl oxygen) conformer was the most stable, consistent with experimental results. A major contribution to the potential energy difference between the *trans* and *cis* conformers was the electrostatic attraction between the carbonyl oxygen and the quaternary amine methyls, which led to increased stabilization of the *trans* isomer with respect to the *cis* isomer. Since in the CHARMm force field, the electrostatics term scales with the dielectric constant, the magnitude of the potential energy difference between the *cis* and *trans* conformers was dependent upon the value of the dielectric, with ϵ= 80 approaching within a factor of two the difference observed experimentally (McGroddy and Oswald, 1993 and see below). The lowest energy configurations of the amide dihedrals deviated from planarity by 8.5°-13.5° in all cases (Table 2 *A*). In addition to the electrostatics term, higher dihedral angle and bond angle energy contributions for the *cis* conformers contributed to the potential energy difference between the *cis* and *trans* amide orientations. In addition, a higher VDW energy contribution in the *trans* conformer was observed, due presumably to the more compact structure formed as a result of the interaction between the quaternary amine methyls and the carbonyl oxygen.

Other dihedrals

All of the rotamers about the C—N(amide)—C—C dihedral were reasonably accessible at room temperature, with potential energy differences of less than 0.1 kcal/mol (data not shown). In contrast, rotamers about the N—C—C—N(+) backbone dihedral showed significant potential energy differences. The potential energies of the TRANS (180°) conformers decreased relative to the GAUCHE (60°) conformers with increasing dielectric (1 to r to 80). This presumably arises from the domination of the electrostatics term in the ϵ = 1 and r cases, and the closer potential approach of the quaternary amine methyls to the carbonyl oxygen in the GAUCHE conformation, particularly when the amide dihedral is *trans*. For a given value of the dielectric, the minimum energy conformers are defined by the dihedral energy which shows minima corresponding to each of the three major conformers (TRANS, GAUCHE, GAUCHE$^-$) of the N—C—C—N(+) backbone for both *cis* and *trans* amide conformations. The differences in potential energy among

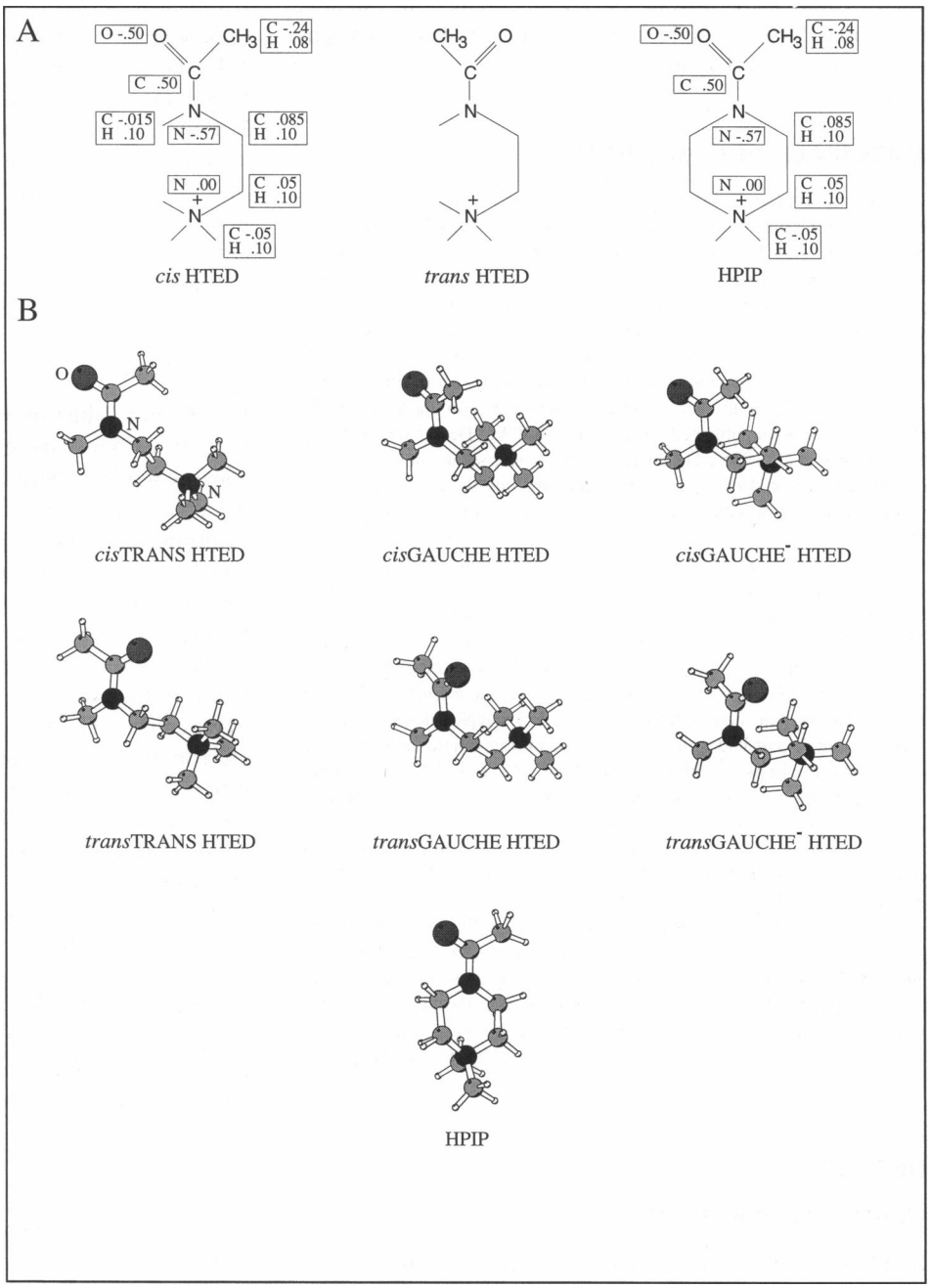

FIGURE 1 A schematic representation of the cholinergic agonist, 1,1-dimethyl-4-acetylpiperazinium iodide (HPIP), and its open-chained derivative, *N,N,N,N'*-tetramethyl-*N'*-acetylethylenediamine iodide (τHTED), in two orientations about the amide bond is shown in (*A*). The charge distribution is shown in the small boxes for each atom. This distribution for *cis* and *trans* HTED was identical. The minimum energy structures (drawn using MolScript (Kraulis, 1991)) of the most populated conformers from the conformational search are shown in (*B*). Nitrogen atoms are shown as black circles, oxygen atoms as dark gray circles, carbon atoms as light gray circles, and hydrogen atoms as small, white circles.

TABLE 1 Potential energies obtained from the conformational search (kcal/mol)

HTED Conformer	$\epsilon = 1$	$\epsilon = r$	$\epsilon = 80$
cT HTED	51.13	31.06	18.34
cG HTED	45.96	29.22	21.07
cG⁻ HTED	46.38	29.97	21.70
tT HTED	39.05	24.95	17.66
tG HTED	39.87	25.95	19.59
tG HTED	39.93	26.22	19.92

these N—C—C—N(+) conformers are then dominated by the bond angle energies, which are always higher in the GAUCHE and GAUCHE⁻ (−60°) backbone orientations than in the TRANS configuration, regardless of the orientation of the amide dihedral. This is due to distortion of the N(amide)—C—C and C—C—N(+) angles by approximately 5° when the N—C—C—N(+) backbone is GAUCHE or GAUCHE⁻. The bond angle energy is usually higher when the N—C—C—N(+) backbone is GAUCHE⁻ (−60°) than when it is GAUCHE (60°), since the N(amide)—C—C angle is slightly more distorted in the former case.

Boltzmann weighting

In order to estimate the population distribution among the six major conformers shown in Fig. 1 *B*, a two dimensional conformational search was performed in which both the amide bond and the N—C—C—N(+) bond dihedrals were varied

TABLE 2 Dihedral angles determined from the conformational search and molecular dynamics simulation (see Fig. 1 for structures)

Molecule	O-C-N-C	N-C-C-N(+)	C-C-N(+)-C	C-N-C-C*
A. Conformational search				
HPIP	9.2°	46.6°	56.0°	−159.1°
*c*T HTED	−173.5°	174.9°	−63.5°	79.5°
*c*G HTED	166.5°	69.6°	−67.0°	59.5°
*c*G⁻ HTED	172.6°	−64.9°	−56.0°	123.5°
*t*T HTED	8.5°	179.0°	−52.3°	88.1°
*t*G HTED	−9.2°	67.9°	−70.1°	64.7°
B. Molecular dynamics simulation (angle ± rms deviation)				
HPIP	−0.42 ± 12.3°	44.4 ± 8.1°	64.6 ± 5.7°	156.8 ± 17.7°
*c*T HTED‡	−173.8 ± 9.3°	173.8 ± 10.6°	−63.1 ± 9.2°	80.1 ± 12.3°
*c*G HTED	165.1 ± 8.2°	70.4 ± 8.4°	−62.4 ± 9.6°	60.8 ± 8.2°
*c*G⁻ HTED‡	168.4 ± 8.6°	−66.3 ± 9.9°	−57.3 ± 9.5°	124.3 ± 8.9°
*t*T HTED	−0.5 ± 10.1°	179.8 ± 13.4°	−60.9 ± 10.3°	91.8 ± 16.7°
*t*G HTED	−3.8 ± 9.7°	69.2 ± 8.7°	−65.3 ± 9.2°	66.4 ± 7.8°

Measured from C(O) in HPIP and from C(amide methyl) in the HTED structures.

‡ During *c*T simulation, a transition to the *c*G⁻ conformer occurred. The data shown for *c*T were taken from the first 48 ps of the trajectory and that for *c*G⁻ were taken from the last 44 ps. The same is true for molecular dynamics data given in all subsequent tables.

in 5° increments for $\epsilon = 80$ ($\epsilon = 1$ and r gave unrealistic values for the *trans/cis* equilibrium). The energy surface is shown in Fig. 2 *A*, with the Boltzmann weighting of the surface in Fig. 2 *B*. Integration of the Boltzmann surface gives a *trans/cis* equilibrium constant of 3.9, slightly smaller than the experimental value of 6.1. A population distribution of 76.6% *trans* TRANS (*t*T), 20.3% *cis* TRANS (*c*T), 1.9% *trans* GAUCHE (*t*G), 1.0% *trans* GAUCHE⁻ (*t*G⁻), and less than 1% *cis* GAUCHE (*c*G) and *cis* GAUCHE⁻ (*c*G⁻) is predicted from these results. This may suggest that, as expected with a formally charged system, solvation effects appear to be important in obtaining the correct free energy difference between the different HTED conformers.

Molecular dynamics simulations

The two lowest energy structures obtained from the conformational search for each of the two amide orientations observed experimentally (*t*T, *t*G, *c*T, and *c*G) were used as starting points for molecular dynamics simulations of HTED in aqueous solution, along with an energy-minimized structure of HPIP. A 100 psec trajectory was generated for each starting orientation and analyzed for torsional transitions and solvation characteristics.

Analysis of bond torsions

The average values and root mean square fluctuations for the torsions in all four HTED simulations and the HPIP simulation are shown in Table 2 along with the initial values obtained from the minimization. Interestingly, the conformations of HTED remained fairly close to the starting positions in all but one of the simulations. During the *c*T simulation, a 120° rotation about the N—C—C—N(+) torsion occurred, leading to a *c*G⁻ structure (N—C—C—N(+) = −60°). The time series for this transition is shown in Fig. 3 *A*. This rotation was accompanied by a large change in the average value of the C—N(amide)—C—C torsion (~40°, shown in Fig. 3 *B*), as well as by a smaller change in the average value of the amide torsion (~20°), consistent with the minimum energy structure of *c*G⁻ determined from the conformational search. The only other torsion angles to exhibit conformational transitions in any of the simulations were the acetyl methyl and amide methyl groups. The similarity in the average values of the C—C—N(+)—C torsion and the lack of rotation about any of the amine methyl groups in any of the simulations are indicative of a fairly rigid structure in this portion of the molecules, possibly due to stable solvation of the positively charged amine methyl groups in both HPIP and HTED.

The C—N(amide)—C—C torsion in HPIP undergoes large deviations throughout the trajectory (Fig. 4 *A*). Visual inspection of the trajectory using QUANTA (Molecular Simulations, Inc.) and calculation of pucker parameters as described by Cremer & Pople (Cremer and Pople, 1975) indicate that the six membered ring of HPIP populates three classes of conformations: twist-boat, chair, and half-chair. The twist-boat conformation is the least populated, with only one 7.5 ps transition to this conformer during the simulation (Fig. 4 *B*; a value of 90° for θ corresponds to a boat conformation). Several transitions to the chair conformer are also seen, but it is not the predominant conformer (Fig. 4 *B*; values of θ near 180° correspond to the chair conformation). During most of the trajectory, the ring populates several conformations that are approximate half-chairs (i.e., the methylene groups and the amide are in the same plane). These correspond to several semi-stable states with θ values between 130° and 165° (Fig. 4 *D*). The amide nitrogen approaches the same plane as the methylene carbons as the value of θ approaches 130°. Due to its sp^2 hybridization, the amide nitrogen favors the planar conformation with a bond angle of 120°. The chair and boat conformers are less stable since the bond angle is deformed by approximately 5° from 120° toward the tetrahedral geometry. On the other hand, the quaternary amine remains fairly rigid and out of the plane of the methylene groups throughout the simulation (note the small deviation in the C—C—N(+)—C torsion in Fig. 4 *D*).

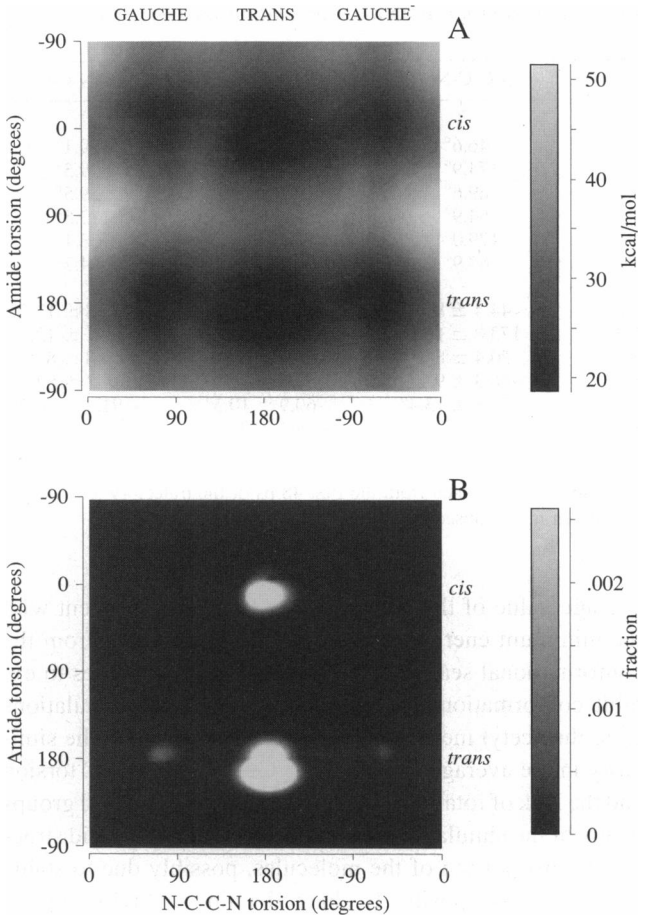

FIGURE 2 The results of the two dimensional conformational search for HTED is shown as (*A*) a potential energy surface and (*B*) a Boltzmann-weighted surface. In (*A*), lighter colors indicate higher energies so that energy minima are represented by the dark areas. For the Boltzmann-weighted surface (*B*), increasing population is goes from dark to light, so that the most populated conformers are indicated as a light surface. The *trans/cis* equilibrium constant was calculated by integrating the surface corresponding to the *trans* conformer and dividing by the integral of the surface for the *cis* conformer. The *trans* integral was defined as the integral over all angles of N—C—C—N(+) from -90° through 180° to 90° (lower half of (*B*)). Likewise, the *cis* integral was defined from 90° through 0° to -90° (upper half of (*B*)). GAUCHE was defined from 0° to 120° of the N—C—C—N(+) torsion, TRANS from 120° to -120°, and GAUCHE⁻ from -120° to 0°.

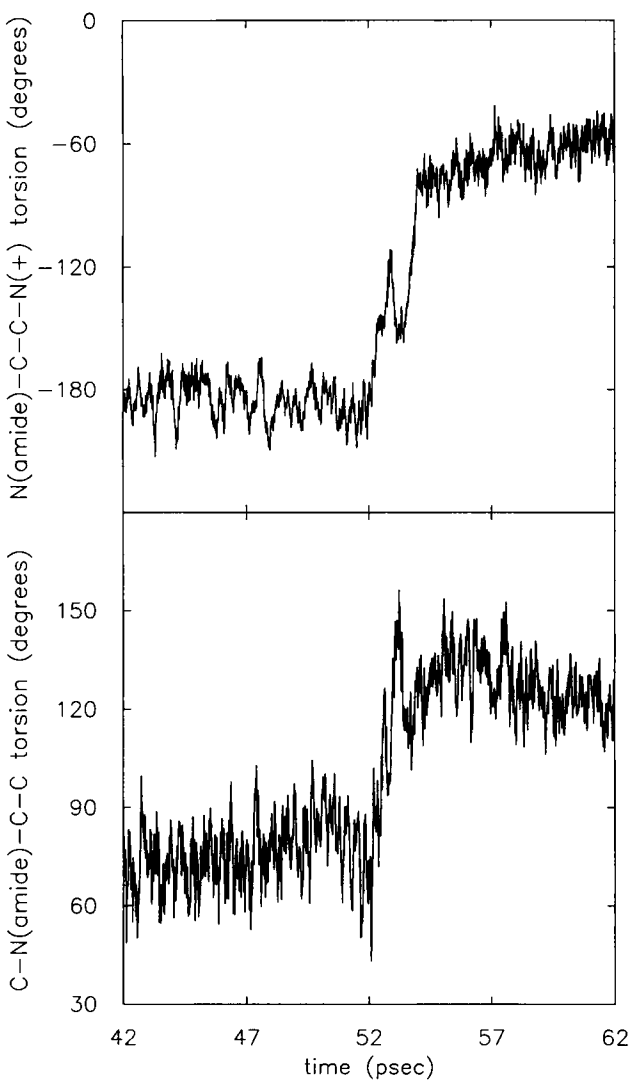

FIGURE 3 Time series for the transition about the N—C—C—N(+) backbone during the *c*T HTED simulation. Shown are (*A*) the N—C—C—N(+) torsion and (*B*) the C—N(amide)—C—C torsion.

This behavior differs significantly from ring structures such as cyclohexane (Cremer and Pople, 1975) in that ring conformations most favored by HPIP are not energetically favored in cyclohexane. This is not due to the interaction with solvent in that a simulation run in vacuum showed similar pucker parameters, the only differences being a higher frequency of transitions between conformers and a greater tendency to form a true half-chair conformer (data not shown). These torsional fluctuations correlate somewhat with changes in the Beers-Reich (Beers and Reich, 1970) distance (i.e., the distance between the amine nitrogen and the van der Waals extension of the carbonyl oxygen) which is thought to be critical for the interaction of the agonist with the nAChR (Fig. 4 *D*). The mean Beers-Reich distance is 6.08 Å and deviations from this value are correlated with transitions to the chair conformation in most, but not all, cases (Fig. 4 *C*).

Calculation of Beers-Reich distance

Beers and Reich (1970), in a classic study of rigid cholinergic agonists suggested that the distance between the amine nitrogen and the van der Waals extension of the carbonyl oxygen ($r_{B\text{-}R}$) should be approximately 5.9 Å for a potent agonist. A comparison of $r_{B\text{-}R}$ as a function of time for each of the structures can be made in order to attempt to predict the orientation of the N—C—C—N(+) dihedral in the active HTED conformer(s). Table 3 shows the average and rms values for $r_{B\text{-}R}$ calculated from the molecular dynamics simulations and for the conformational search described above. The average $r_{B\text{-}R}$ values computed from the simulations are not significantly different from the $r_{B\text{-}R}$ values of the minimized structures (Table 3 *A*). For HTED, the results clearly

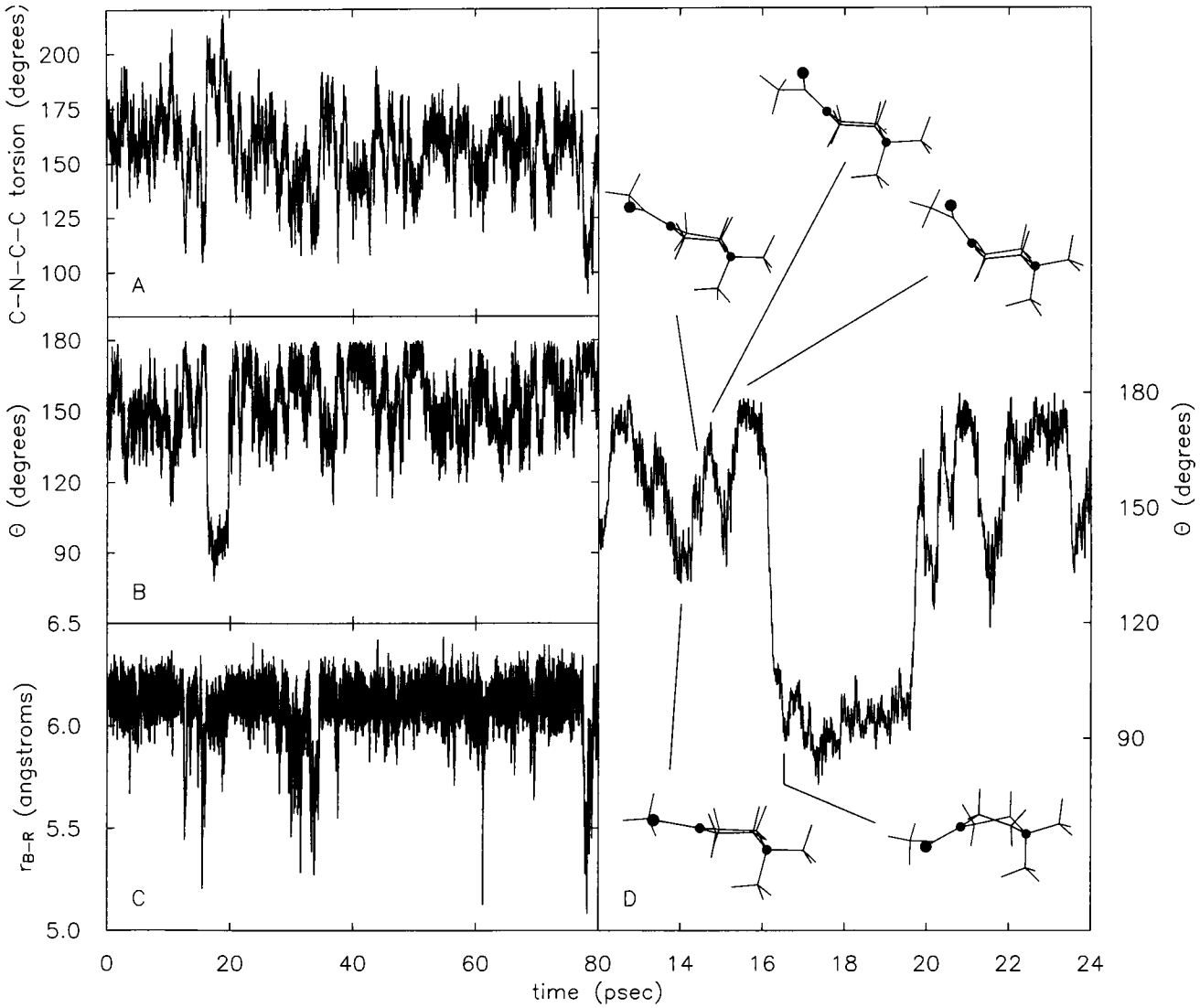

FIGURE 4 Dynamics observed during the HPIP simulation. (*A*) The C—N(amide)—C—C torsion is shown and reflects the dynamics at the amide portion of the molecule. (*B*) A time series for the pucker parameter, θ (Cremer and Pople, 1975), is shown. This parameter can be used to describe a chair (0° and 180°), boat (90°), or intermediate conformers. (*C*) A time series showing the r_{B-R} (Beers-Reich distance) for HPIP. (*D*) This time series represents a magnification of a portion of (*B*) illustrating the semi-stable states forming an approximate half-chair. The structures shown are taken from the indicated point in the trajectory and are drawn using MolScript (Kraulis, 1991). The nitrogen atoms are shown as black circles and the oxygen atoms as gray circles. Note that the bond between the carbon and oxygen in each structure is a double bond.

indicate that the amide dihedral must be *cis* and the N—C—C—N(+) backbone must be in a GAUCHE (±60°) orientation in order to fit the proposed Beers and Reich pharmacophore. The r_{B-R} is too short when the amide dihedral is *trans*, and too long in the *c*T conformer. These results are also consistent with the observed potency of HPIP, since the average r_{B-R} is consistent with the pharmacophore and the N—C—C—N(+) backbone in HPIP is near GAUCHE and cannot achieve a TRANS orientation without severe angle and bond strain. Thus, only a subset of HTED conformers is in the correct conformation to be recognized by the nAChRs.

Because the affinity of HPIP and HTED for nAChRs may also be affected by solvation, we investigated the distribution of water around each of the solutes during the simulations. In order to compare the solvation characteristics, the radial distribution functions (*rdf*s), $g_{xy}(r)$, were calculated for the bulk water and for the interaction of the water oxygens and hydrogens with each nonhydrogen atom in the solute. These functions give the probability of finding an atom of type *y* at a distance *r* from an atom of type *x*. For bulk water (g_{OO}, g_{OH}, g_{HH}), *rdf*s were similar to previously published results (Jorgensen et al., 1983). The distribution of water around each solute atom was then investigated.

The radial distribution of water around the polar carbonyl oxygen is shown in Fig. 5. The *rdf*s do not differ dramatically among the six structures (HPIP and *c*G, *t*G, *c*G$^-$, *c*T, and *t*T HTED). In each case the first peak in $g_{OO}(r)$ occurs at 2.8 Å and that of $g_{OH}(r)$ at 1.95 Å. This indicates that, as expected, the carbonyl oxygen is acting as a hydrogen bond acceptor. The *rdf*s for the amine

TABLE 3 Beers Reich distances (Å) determined from molecular dynamics simulations and from minimum energy structures obtained from the conformational search

Molecule	Conformational search	Molecular dynamics
HPIP	6.18	6.08 ± 0.16
*c*T HTED	7.39	7.38 ± 0.13
*c*G HTED	6.02	6.05 ± 0.25
*c*G⁻ HTED	6.05	6.01 ± 0.26
*t*T HTED	4.68	4.78 ± 0.45
*t*G HTED	4.99	4.83 ± 0.38
*t*G⁻ HTED	4.86	n.d.

nitrogen are shown in Fig. 6. The peaks in $g_{NO}(r)$ and $g_{NH}(r)$ for all of the structures occurs at 4.55 to 4.65 Å, suggesting no preferential orientation of the water with respect to the amine nitrogen. This is due to the fact that the water is associated with the methyl groups bonded to the amine, although the shoulders seen in $g_{NO}(r)$ at approximately 4.1 Å are probably due to water molecules positioned between two methyl groups.

To obtain the coordination numbers for several of the solute atoms, the number of water oxygens within a cutoff determined by the first minimum in the *rdf* was averaged over the simulation (Table 4). For both the carbonyl oxygen and the quaternary amine, the *cis* TRANS conformer of HTED was more solvated than the other conformers. This is consistent with the more extended conformation (as seen in Fig. 1) and indicated by the larger $r_{B\text{-}R}$ (Table 3). Furthermore, the amine methyl groups in the GAUCHE conformers are differentially solvated; whereas, those of the TRANS conformers are solvated to approximately the same extent. The differential solvation is probably due to the more compact structure of GAUCHE HTED, where one or more of the amine methyl groups appears to remain near the backbone of the molecule due to electrostatic attraction with the carbonyl oxygen. When the N—C—C—N(+) backbone is TRANS, all of the amine methyl groups are more evenly exposed to the solvent. This was tested by determining the number of water oxygens within the first hydration shell of amine methyl groups closest, intermediate, and furthest at any given time from the carbonyl methyl (the distance from the carbonyl methyl is a more reliable indication of the proximity to the backbone of the molecule). Clearly, in the case of the GAUCHE conformers, one of the methyl groups is shielded by the backbone of the molecule; whereas, in the case of the TRANS conformers, the methyls are equally solvated. Interestingly, a significant fraction of the waters which associate with the carbonyl oxygen are also within the primary solvation shell of the amine nitrogen in *t*G (0.24), *t*T (0.24), *c*G⁻ (0.16), and *c*G HTED (0.25). In approximately half of the cases, the water appears to bridge between the two solute atoms, with a water proton forming a hydrogen bond with the carbonyl oxygen. This arrangement is precluded in *c*T HTED because of the greater distance between and relative orientation of the carbonyl oxygen and quaternary amine.

The total number of water molecules in the primary solvation shell was determined for each HTED conformer as well as for HPIP (Table 5) as described above for individual solute atoms. The most significant differences for the HTED

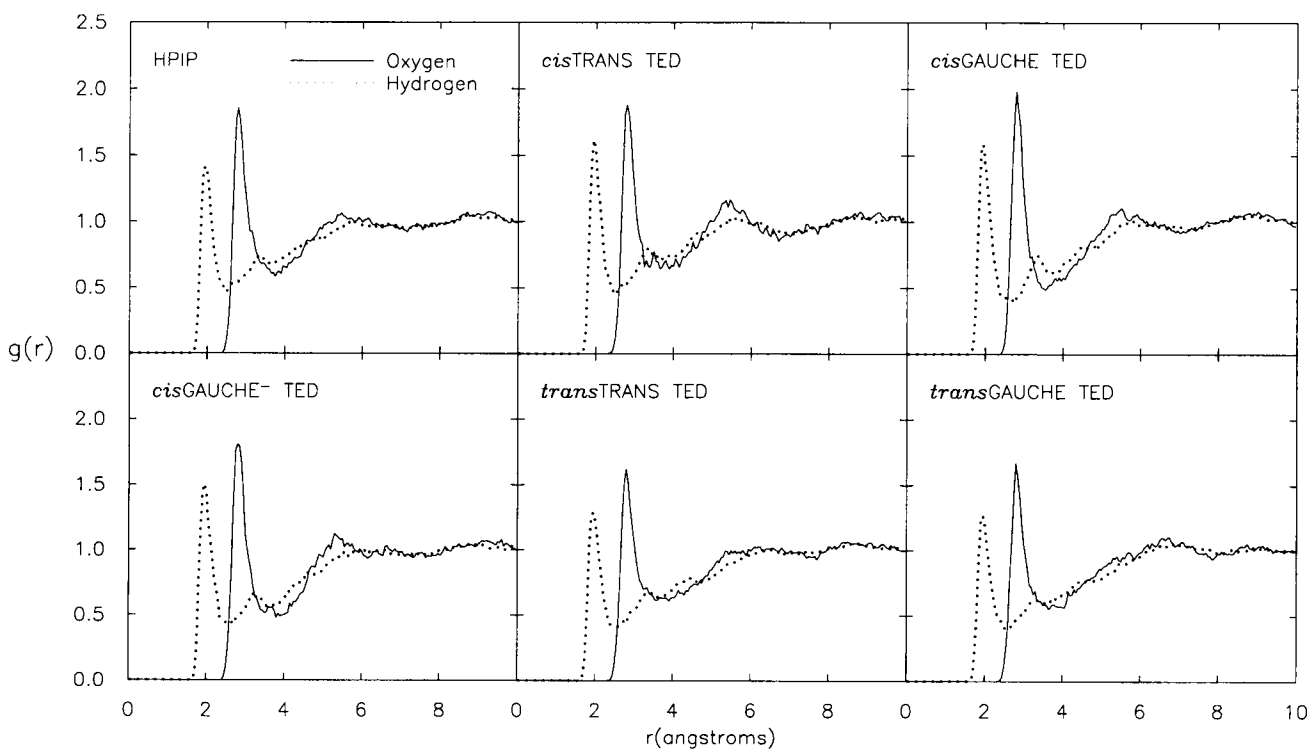

FIGURE 5 Radial distribution functions $g_{OO}(r)$ (solid lines) and $g_{OH}(r)$ (dotted lines) for the carbonyl oxygen and water atoms.

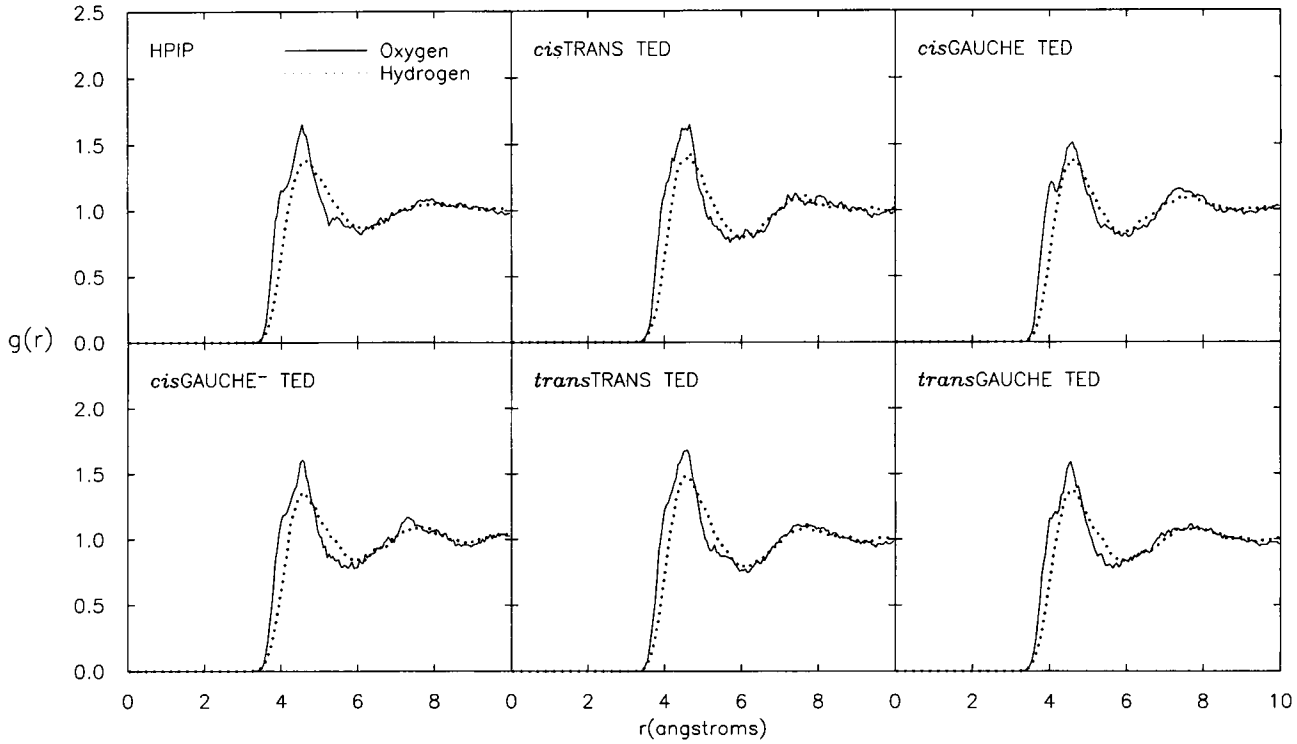

FIGURE 6 Radial distribution functions $g_{NO}(r)$ (solid lines) and $g_{OH}(r)$ (dotted lines) for the quaternary amine nitrogen and water atoms.

TABLE 4 Average coordination numbers for selected solute atoms

Atom	HPIP	*c*T	*c*G	*c*G⁻	*t*T	*t*G
O	4.1 ± 1.1	4.1 ± 1.1	3.8 ± 1.1	3.8 ± 1.0	3.7 ± 1.2	3.6 ± 1.1
N(+)	21.1 ± 2.0	23.8 ± 2.1	20.4 ± 2.0	20.0 ± 1.9	21.3 ± 2.2	20.1 ± 1.8
C(N+)-CH_3)	6.6 ± 1.2	6.5 ± 1.2	5.7 ± 1.2	6.6 ± 1.3	6.8 ± 1.4	5.4 ± 1.2
	7.1 ± 1.3	7.4 ± 1.5	7.4 ± 1.4	7.5 ± 1.4	7.3 ± 1.5	7.3 ± 1.4
	4.5 ± 1.1*	6.8 ± 1.3	6.8 ± 1.2	5.7 ± 1.2	7.1 ± 1.3	6.6 ± 1.3
Far‡		7.1 ± 1.4	7.2 ± 1.4	7.5 ± 1.4	7.2 ± 1.4	7.2 ± 1.3
Intermediate		6.8 ± 1.4	7.1 ± 1.3	6.5 ± 1.3	6.9 ± 1.4	6.7 ± 1.3
Close		6.8 ± 1.3	5.6 ± 1.2	5.7 ± 1.3	7.1 ± 1.3	5.4 ± 1.2

* CH_2 in HPIP.

‡ far, intermediate, and close indicate the quaternary amine methyl furthest, intermediate, and closest to the amide methyl carbon at any given time in the simulation.

TABLE 5 The average primary solvaiotn shells of each conformer calculated from the molecular dynamics simulations

Molecule	Number of water molecules	Solvent-accessible surface area (Å)
HPIP	33.1 ± 2.22	334
*c*T HTED	38.5 ± 2.67	361
*c*G HTED	37.0 ± 2.43	349
*c*G⁻ HTED	36.3 ± 2.30	344
*t*T HTED	38.2 ± 2.45	361
*t*G HTED	36.6 ± 2.27	344

structures are between the TRANS and GAUCHE conformers of HTED, while the orientation about the amide dihedral does not appear to affect the solvation significantly. These results are consistent with the idea that HTED is in a more compact conformation with less solvent-accessible surface area when the N—C—C—N(+) backbone is GAUCHE. In addition, HPIP is less solvated than all of the HTED conformers by three to five water molecules on average. The reduced solvation of HPIP is due to the fact that two of the methyl groups in HTED are replaced by methylene groups in HPIP, and each methylene group is less solvated by approximately two water molecules than the methyl groups in HTED. These solvation differences suggest that more energy may be required to desolvate HTED prior to binding than HPIP.

Trans/cis equilibrium constant

The average total energies and their components obtained from the molecular dynamics simulation are shown in Table 6. Also shown are the individual potential energy contributions partitioned into intramolecular solute energies and contributions arising from the solvent-solute interactions. Clearly, the solvent-solvent interactions

TABLE 6 Average values and rms fluctuations of the energies from the molecular dynamics simulations (all values in kcal/mol except for temperature, which is expressed in Kelvin)

Component	HPIP	*c*T	*c*G	*c*G$^-$	*t*T	*t*G
Total energy	−4297.7 ± .07	−4299.2 ± .06	−4302.6 ± .06	−4299.2 ± .05	−4294.9 ± .09	−4303.3 ± .06
Temperature (K)	299.1 ± 6.2	298.4 ± 6.1	297.8 ± 6.3	298.2 ± 6.1	299.5 ± 6.1	298.2 ± 6.2
All interactions						
Potential energy	−5207.1 ± 23.3	−5208.0 ± 21.7	−5209.6 ± 18.8	−5207.2 ± 19.5	−5206.8 ± 21.1	−5212.0 ± 19.6
E(Bond)	10.9 ± 2.3	11.2 ± 2.5	11.5 ± 2.4	11.3 ± 2.3	11.0 ± 2.4	11.5 ± 2.4
E(Angle)	15.8 ± 2.8	17.7 ± 3.1	18.2 ± 3.1	18.7 ± 3.0	16.7 ± 3.1	17.9 ± 3.1
E(Dihedral)	4.3 ± 1.4	3.3 ± 1.3	4.1 ± 1.4	3.5 ± 1.4	2.7 ± 1.1	2.7 ± 1.2
E(Improper)	1.2 ± 1.1	.7 ± .7	1.4 ± 1.0	1.2 ± .9	.8 ± .8	1.0 ± 1.0
E(Electrostatic)	−5806.8 ± 71.0	−5810.8 ± 87.1	−5810.0 ± 70.2	−5807.1 ± 65.3	−5803.4 ± 71.9	−5813.0 ± 69.8
E(VDW)	567.6 ± 30.4	569.9 ± 30.6	565.1 ± 30.6	565.1 ± 30.1	565.5 ± 29.6	568.0 ± 29.4
Solute only*						
Potential energy	60.4 ± 3.1	68.0 ± 3.3	62.8 ± 3.2	62.2 ± 3.0	56.6 ± 4.0	55.5 ± 3.6
E(Bond)	7.4 ± 2.3	7.7 ± 2.5	8.0 ± 2.4	7.8 ± 2.3	7.5 ± 2.4	7.9 ± 2.4
E(Electrostatic)21.9 ± 1.3	29.7 ± 1.1	22.4 ± 1.5	22.2 ± 1.6	19.7 ± 2.3	17.1 ± 1.9	
E(VDW)	9.8 ± 2.2	8.9 ± 2.3	8.9 ± 2.3	8.8 ± 2.3	9.2 ± 2.3	9.0 ± 2.4
Solute-solvent interactions‡						
Potential energy	−117.7 ± 8.2	−122.5 ± 8.4	−113.3 ± 8.1	−113.5 ± 8.1	−104.6 ± 9.5	−104.0 ± 8.1
E(Electrostatic)	−97.4 ± 8.3	−100.9 ± 8.6	−92.3 ± 8.4	−92.2 ± 8.2	−83.3 ± 8.4	−82.7 ± 8.3
E(VDW)	−20.4 ± 2.3	−21.2 ± 2.4	−21.1 ± 2.2	−21.8 ± 4.0	−21.3 ± 2.3	

* The angle, dihedral, and improper energies are identical with the case for which all interactions are considered.

‡ The angle, dihedral, and improper energies are identical with the case for which all interactions are considered; and the bond energy is identical with the solute only case.

contribute significantly to the total potential energy of the system, largely through the electrostatics term. Considering only the intramolecular solute potential energies, the results obtained are similar to the energy minimization with $\epsilon = 1$. That is, the *trans* conformers were favored by greater than 5 kcal/mol over the *cis* conformers, which would predict a *trans/cis* equilibrium constant (obtained by multiplying by a Boltzmann factor) of more than 6×10^4, clearly not consistent with experimental observations. On the other hand, the potential energy of solvent-solute interaction includes a very favorable electrostatics term for the *cis* conformers, which seems to arise from the increased exposure of the carbonyl oxygen to solvent. Considering both the intramolecular solute energies and the solvent-solute interaction energies, the *trans/cis* equilibrium constant is decreased to approximately 6×10^{-5}, also inconsistent with experimental results. However, when the potential energies of the entire system were multiplied by a Boltzmann factor in order to obtain estimates for the *trans/cis* equilibrium constant, a result of 51.6 was obtained, a value 8.5-fold greater than the experimental value of 6.1. Note, however, that the rms fluctuations are fairly large (Table 6). The difference between the calculated and experimental ratios reflects the fact that it is particularly difficult to calculate free energies from molecular mechanics calculations. Incomplete sampling, particularly for high energy states, leads to poor statistical convergence for simulations of finite length. In addition, further quantitative errors arise from inaccuracies associated with the use of empirical potential energy functions to model the solute and liquid water. Furthermore, the shifting algorithm, used in these simulations to truncate long range electrostatic interactions, will affect solute-solvent and solvent-solvent binding energies and may result in additional deviations from experimental values. However, since the results are reported for individual conformational states, the intramolecular energies of the solute and the interaction energies of the solute with the solvent have very likely converged. These results would predict a solution population distribution of 98% *t*G HTED and 1.6% *c*G HTED, with the *t*T, *c*G$^-$ and *c*T conformers less than 1% populated. In contrast, the results of the conformational search suggest that the TRANS conformers would be more greatly populated.

DISCUSSION

Energies

Neither the conformational search nor the molecular dynamics simulations were able to reproduce exactly the free energy difference between HTED conformers measured in aqueous solution. The results from the conformational search indicate that in the isolated molecule, HTED is most stable in a *trans/*TRANS conformation. The equilibrium population distribution calculated from these results, however, would lead to a *trans/cis* equilibrium constant of 3.9 with $\epsilon = 80$, and over 1000 with $\epsilon =$ r and $\epsilon = 1$, while the observed experimental value is 6.1 (McGroddy and Oswald, 1993). The actual local dielectric in solution is probably less than 80 but greater than what was obtained by using $\epsilon =$ r. The molecular dynamics simulations indicate that the inclusion of solvent leads to a significant lowering of the potential energy of *t*G HTED as compared to *t*T HTED, mainly due to the electrostatics term. The *trans/cis* ratio computed from the average potential energies of the four starting conformers (*c*T, *c*G, *t*T, *t*G and *c*G$^-$) is 51.6, in this case 8.5-fold greater than the ratio observed experimentally. While the simulations approach the correct order of magnitude of the *trans/cis* ratio, some discrepancy exists between the predicted and observed values. Nevertheless, the results clearly indicate that the electrostatic

contribution of the solvent plays a major role in determining the conformation of this molecule. The experimental NMR data is not conclusive in determining the orientation of the N—C—C—N(+) backbone in HTED, since NOEs are difficult to measure on a molecule of this size. Further work will need to be done in the form of NMR measurements on isotopically labeled HTED molecules in conjunction with free energy simulations in order to clearly determine the equilibrium population distribution.

Structures and dynamics

The molecular dynamics simulations showed that HPIP is not a rigid molecule as originally thought, but that it undergoes significant dynamics at the acetyl end while the quaternary amine methyls remain rigid due to stable solvation. The piperazinium ring restricts the N—C—C—N(+) backbone to a GAUCHE-like orientation, so it is easy for HPIP to achieve the correct conformation to bind to the nAChRs. The quaternary amine portion of HPIP is very rigid, however, with a stable solvation structure. HTED is also a fairly rigid molecule, with the average torsion values over 100 psec very close to the values measured in each minimized structure. One transition about the N—C—C—N(+) dihedral was observed, but the only other rotations observed in any of the simulations were by the acetyl methyl or amide methyl groups. None of the quaternary amine methyl groups underwent any rotation during any of the simulations.

Only HPIP and the two *cis* GAUCHE conformers of HTED appear to fulfill the Beers and Reich criteria for agonists. The *trans* HTED conformers are too compact, while *c*T HTED is too extended. The rms deviations from the average carbonyl oxygen-amine nitrogen distances are very small, again indicating that the structures are very stable. Thus, only a percentage of HTED in solution is available for binding to the nAChRs. Isomerization about the amide bond is slow at room temperature and will impact the binding kinetics, but the energy barrier to rotation about the N—C—C—N(+) dihedral is probably not very high, since a transition was observed in these relatively short simulations. Free rotation about this dihedral could lead to a greater loss of entropy upon binding of HTED as compared to HPIP; however, qualitatively HPIP does not appear to be more rigid than HTED during these simulations.

Solvation

The solvation characteristics of these molecules were compared in several ways, since differences in the energetics of desolvation might partially explain the differences in potency between HPIP and HTED. The pair distribution functions for the interaction of water with the carbonyl oxygen and the quaternary amine nitrogen were compared, and found to be relatively similar. HPIP and *c*T HTED appear to be slightly more solvated at the carbonyl oxygen than the remainder of the HTED derivatives, probably due to shielding by the backbone of the molecule in the latter cases. A larger difference was seen when the solvation of the quaternary amine methyls was compared. When the backbone of HTED is in the GAUCHE configuration, the three methyl groups are solvated differentially due to shielding by the remainder of the backbone. This is not the case in HPIP or when the HTED backbone is TRANS, where the amine methyls are more evenly solvated. Thus, the overall solvation of the groups carrying the positive charge is higher in the TRANS HTED conformers than in the GAUCHE conformers or HPIP.

Additional differences in the solvation of these molecules were observed by comparing the average number of water molecules in the primary solvation shell of each structure. The two TRANS conformers of HTED were the most solvated, probably due to the decreased shielding of the quaternary amine methyls by the N—C—C—N(+) backbone. The GAUCHE conformers have approximately two fewer water molecules in the primary solvation shell on average. HPIP is less solvated than any of the GAUCHE HTED structures by 3 to 5 water molecules. This could contribute to the differences in potency between HPIP and HTED, since it will probably take less energy to desolvate HPIP than any of the HTED conformers. These results are consistent with solvent-accessible surface area calculations on the minimized structures, in which HPIP has from 10 $Å^2$ to 23 $Å^2$ less solvent accessible surface area than any of the HTED structures (Table 5).

The differences in the primary solvation shell may also contribute to the free energy differences between the HTED conformers. Since the TRANS conformers are more solvated, there may be an unfavorable entropic contribution to the free energies of *c*T and *t*T HTED as compared to *c*G and *t*G HTED. This suggests that the predominant HTED conformer in solution has a GAUCHE backbone. Acetylcholine has also been shown to have a GAUCHE backbone in solution, so this result would not be unexpected.

CONCLUSIONS

Energy minimization and molecular dynamics simulations support the notion that the major potency differences between HPIP and HTED are due to differences in solution structure. Only the *c*G or *c*G^- conformations exhibit the appropriate Beers-Reich distance (Beers and Reich, 1970) which has been postulated to be necessary for receptor activation. Thus, only a small percentage of HTED molecules in solution may be capable of interacting with nAChRs. It is not clear from these results whether or not there is an entropic contribution to the difference in the free energies of binding between HPIP and HTED, but differences in the solvation of these molecules probably plays a role in their different biological activities. Also, these results appear to strengthen the conclusion that the active conformation of ACh is not TRANS (McGroddy et al., 1993; Wilson et al., 1991) as has been suggested (Behling et al., 1988) and very likely that ACh must have a GAUCHE backbone when bound to the nAChR.

The authors would like to thank Kenzabu Tasaki and Rebecca Schmidt for helpful discussions.

This work was supported by NIH Grant RO1 NS 18660, NSF Grant BNS-9021407, and Molecular Simulations, Inc. Kathleen A. McGroddy was supported by the NIH predoctoral training grant T32GM08267.

REFERENCES

Beers, W. H., and E. Reich. 1970. Structure and activity of acetylcholine. *Nature (Lond.)* 228:917–922.

Behling, R. W., T. Yamane, G. Navon, and L. W. Jelinski. 1988. Conformation of acetylcholine bound to the nicotinic acetylcholine receptor. *Proc. Natl. Acad. Sci. (U.S.A.)* 85:6721–6725.

Cremer, D., and J. A. Pople. 1975. A general definition of ring puckering coordinates. *J. Am. Chem. Soc.* 97:1354–1358.

Dewar, M. J. S., and E. G. Zoebisch. 1988. Extension of AM1 to the halogens. *J. Mol. Struct.* 180:1–21.

Dewar, M. J. S., E. G. Zoebisch, E. F. Healy, and J. J. P. Stewart. 1985. AM1: A new general purpose quantum mechanical molecular model. *J. Am. Chem. Soc.* 107:3902–3909.

Gund, T. M., C. E. Spivak, J. A. Waters, R. F. Liang, and J. Yadav. 1986. Structural and electronic requirements for potent agonists at a nicotinic receptor. *Abstr. Neurosci.* 12:730.

Jorgensen, W. L., J. Chandrasekhar, J. D. Madura, R. W. Impey, and M. L. Klein. 1983. Simple potential functions for water. *J. Chem. Phys.* 79: 926–935.

Jorgensen, W. L., and J. Gao. 1986. Monte Carlo simulations of the hydration of ammonium and carboxylate ions. *J Chem. Phys.* 90: 2174–2182.

Jorgensen, W. L., and C. J. Swenson. 1985. Optimized intermolecular potential functions for amides and peptides. Structure and properties of liquid amides. *J. Am. Chem. Soc.* 107:569–578.

Kraulis, P. J. 1991. MolScript–a program to produce both detailed and schematic plots of protein structures. *J. Appl. Crystallogr.* 24:946–950.

McGroddy, K. A., A. A. Carter, M. M. Tubbert, and R. E. Oswald. 1993. Analysis of cyclic and acyclic nicotinic cholinergic agonists using radioligand binding, single channel recording, and nuclear magnetic resonance. *Biophys. J.* 64:325–338.

McGroddy, K. A., and R. E. Oswald. 1993. Solution structure and dynamics of cyclic and acyclic cholinergic agonists. *Biophys. J.* 64:314–324.

Ryckaert, J. P., G. Cicotti, and H. J. C. Berendsen. 1977. Numerical integration of the Cartesian equations of motion of a system with constraints: molecular dynamics of n-alkanes. *J. Comp. Phys.* 23:327–341.

Spivak, C. E., T. M. Gund, R. F. Liang, and J. A. Waters. 1986. Structural and electronic requirements for potent agonists at the nicotinic receptor. *Eur. J. Pharmacol.* 120:127–131.

Spivak, C. E., J. A. Waters, and R. S. Aronstam. 1989. Binding of semirigid nicotinic agonists to nicotinic and muscarinic receptors. *Mol. Pharmacol.* 36:177–184.

Tasaki, K., S. McDonald, and J. W. Brady. 1993. Observations concerning the treatment of long-range interactions in molecular dynamics simulations. *J. Comput. Chem.* 14:278–284.

van Gunsteren, W. F., and H. J. C. Berendsen. 1977. Algorithms for macromolecular dynamics and constraint dynamics. *Mol. Phys.* 34:1311–1327.

Wilson, K. J., M. G. McNamee, and W. L. Peticolas. 1991. The time dependent UV resonance raman spectra, conformation, and biological activity of acetylcholine analogues upon binding to acetylcholine binding proteins. *J. Biomolec. Struct. Dynam.* 9:489–509.